Cement and Concrete Research 40 (2010) 802–809

Contents lists available at ScienceDirect

Cement and Concrete Research

journal homepage: http://ees.elsevier.com/CEMCON/default.asp

Fiber–matrix interaction at early ages of concrete with short fibers

Gonzalo Barluenga *

Departamento de Arquitectura, Escuela Técnica Superior de Arquitectura y Geodesia, Universidad de Alcalá, C. Santa Úrsula, 8. Alcalá de Henares-28801, Madrid, Spain

ARTICLE INFO

Article history:
Received 2 March 2009
Accepted 27 November 2009

Keywords:
Short glass fiber
Early age shrinkage (C)
Crack Detection (B)

ABSTRACT

The inclusion of small amounts of short fibers has demonstrated to be an effective solution to control cracking due to drying shrinkage of concretes at early ages. The key point of fiber effectiveness is their capacity to sew the crack sides, preventing crack opening, because cracking of concrete matrix induces fiber actuation. In this paper, fiber–matrix interaction is analyzed considering different amounts (from 600 to 1200 g/m^3) and lengths (6, 12 and 18 mm) of alkali-resistant (AR) glass fibers and fiber coating effect. The combination of experimental results previously published and analyses with simple FE models allows for better understanding of early age concrete behavior. As concrete mechanical capacity develops with age, while fibers have full properties before being included in concrete matrix, the interphase between matrix and fibers evolves during setting and hardening, and affects cracking control effectiveness, due to stresses induced by fibers into the matrix during concrete hydration.

1. Introduction

As a result of the setting and hardening process, physical and mechanical properties of concrete develop with age. At early ages, between 2 and 10 h, chemical processes, such as cement hydration, and physical phenomena, as settlement, occur, producing water displacement and hydration product displacements (which, in turn, produce new water displacements).

The chemical reactions of concrete depend on environmental conditions. The macroscopic effects of cement hydration consist on a change from plastic to rigid behavior, a dimensional change due to autogenous shrinkage and the development of mechanical properties.

It has been proved that the mechanical properties evolution and the cement hydration rate are related [1]. After 10 h, a maximum value of rate of heat evolution takes place [2] and a change in the mechanical behavior has been described [3], reaching a minimum value of tensile strain at failure. Therefore, before 10 h of age this value decreases, and when longer time has passed, the value decreases.

Considering the mechanical parameters evolution, Young modulus has been applied first, then the tensile strength and later the compressive strength [1].

In addition, concrete shows creep when subjected to a displacement restraint, achieving a tensile stress relaxation (creep) which can reach 50% of instantaneous stresses at early ages [4]. Concrete creep has been observed to be beneficial to reduce cracking risk, because of the relaxation of tensile stress produced by shrinkage at early age [1,4,5].

The water movements through the concrete matrix at early ages also determine concrete behavior, depending on the ease of water displacement in relation to solid particles and the bonding stresses. The main macroscopic effects of water movement are early age drying shrinkage and a loss of mass due to evaporation [3].

Depending on the sequence of phenomena occurrence, shrinkage (autogenous and drying) can produce cracking at early ages, whether tensile strength is overcome. Although chemical and physical phenomena are closely related, the macroscopic effects do not occur simultaneously. It has been observed that, although cracking can occur due to shrinkage, both phenomena are not linearly related [6]. Self compacting concrete samples (SCC) presented larger drying shrinkage than conventional concrete but similar cracking at early ages.

The inclusion of low amounts of dispersible short fibers aims to control cracking due to concrete shrinkage at early ages and has been demonstrated to be an effective solution [6–9]. As the amount of fibers incorporated is very low (around 0.1% volumetric fraction, VF), it cannot be considered as a macroscopic mechanical reinforcement, but a local reinforcement which acts after concrete matrix cracks. Furthermore, the dispersive ability of the fibers produces a randomized distribution of single filaments inside the concrete matrix [6].

The short fibers used are made of materials that do not react with cement hydration products (at least at early ages), as polypropylene or alkali-resistant (AR) glass fibers, and their properties remain constant (unlike concrete) during setting and hardening of concrete. On the other hand, their inclusion does not modify concrete shrinkage significantly [6].

As fibers are randomly distributed in the concrete matrix, cracks can reach a perpendicular fiber which can stop crack growth, when propagating through concrete. Fiber cracking control capacity depends

* Tel.: +34 91 883 92 39; fax: +34 91 883 92 76.
E-mail address: gonzalo.barluenga@uah.es.

0008-8846/$ – see front matter © 2009 Elsevier Ltd. All rights reserved.
doi:10.1016/j.cemconres.2009.11.014

on fiber mechanical properties, shape and dimensions: fiber material and fiber section (usually circular) determine its tensile strength, and its length, as well as the fiber to hydrated cement paste bonding capacity, also called interface, and the limit fiber pull-out strength.

The concept of interface is considered in the literature as referring to a molecular level (fundamental adhesion) and a microstructural level (single fiber) [10]. Interface formation and performance are also modified by fiber coating (also called sizing), softening interfacial bonds and improving fiber–matrix compatibility [11,12]. As fiber–matrix interface is in formation when cracking begins, its pull-out strength development determines fiber efficiency at early ages.

Glass–fiber length has been described as a less important part of interface strength, since the pull-out strength does not increase significantly over 1 mm interfacial length [10]. Furthermore, fiber length has been reported to decrease significantly fiber–matrix toughness, as longer fibers fail mainly due to fiber fracture, which consumes less fracture energy than fiber pull-out [13].

In a previous research, a study on cracking control effectiveness, due to drying shrinkage at early age, was reported [6]. The paper refers to the inclusion of two types of dispersible short alkali-resistant (AR) glass fibers in a self compacting concrete (SCC) and two conventional concretes. Two main conclusions were drawn: cracking control ability of low amounts of short fibers was very similar for different types of concrete (standard and SCC), and higher VF of fibers did not improve cracking control, but in some cases, efficiency even decreased.

Fig. 1 shows the cracked area and maximum crack length measured on SCC and standard concrete specimens modified with different amounts of both types of AR-glass fibers under study [6]. As far as only two specimens of each fiber VF and fiber type were tested, no variability studies could be done. SCC and standard concrete without fibers presented similar values of cracked area, though maximum crack length greatly differed (experimentally measured average error was under $\pm 0.01\%$ in all cases).

The inclusion of low VF of AR-glass fiber (600 g/m^3) produced a minimum value of both cracked area and maximum crack length. For fiber amounts around 900–1000 g/m^3, an unexpected decrease of cracking control effectiveness was observed, whereas maximum crack length remained practically constant. The decrease on the cracking control ability was measured in three out of four cases, considering two types of dispersible fibers (W70 and HD) and two types of concrete (conventional and SCC).

As it happens with any type of short fibers when added to fresh concrete, two main patterns of relative positions between fibers and cracks were observed. When a crack grows perpendicular to a fiber, its cracking control ability is high and can limit crack growth. If the crack appears parallel to a fiber, as can be observed in the three micrographies of Fig. 2, it can progress easier, producing detachment between fiber and concrete matrix. It can be also observed that filaments that form the dispersible AR-short glass fibers effectively get dispersed (all the visible filaments are alone on the surface of the concrete matrix).

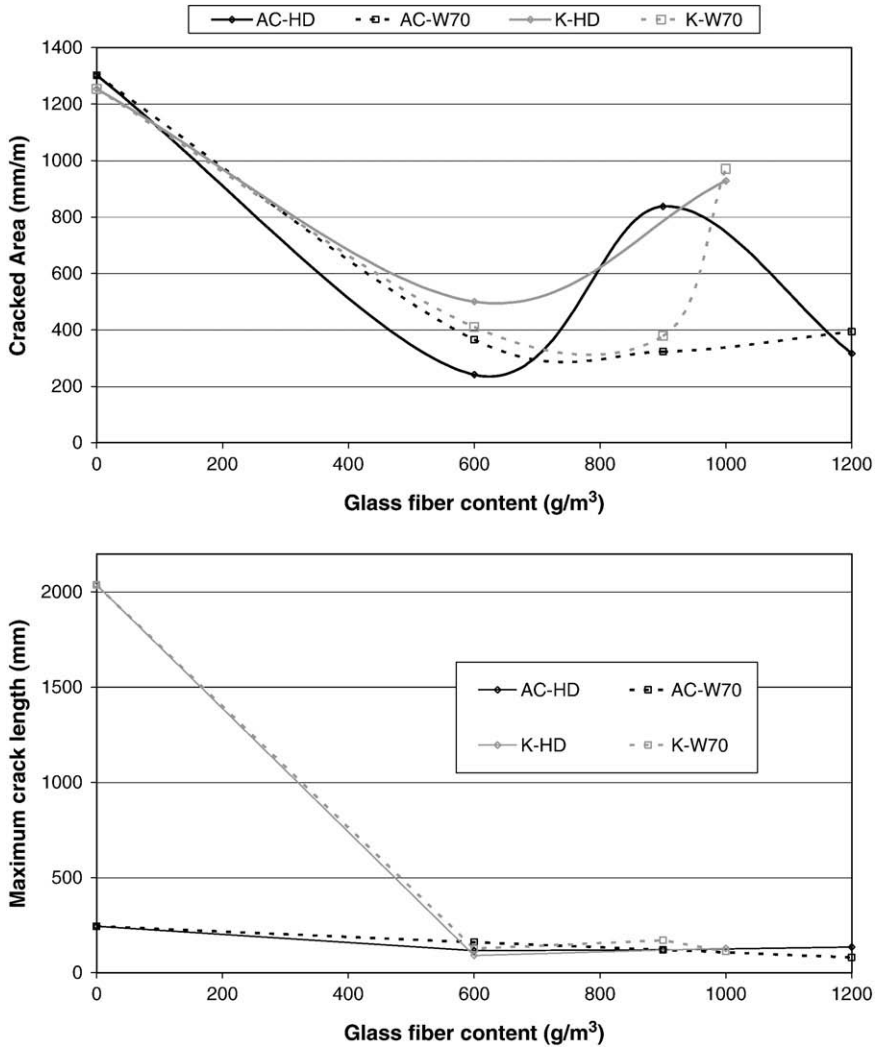

Fig. 1. Cracked area and maximum crack length of SCC (*AC*) and standard concrete (*K*) specimens modified with low amounts of two types of short AR-glass fibers (*HD* and *W70*) [6].

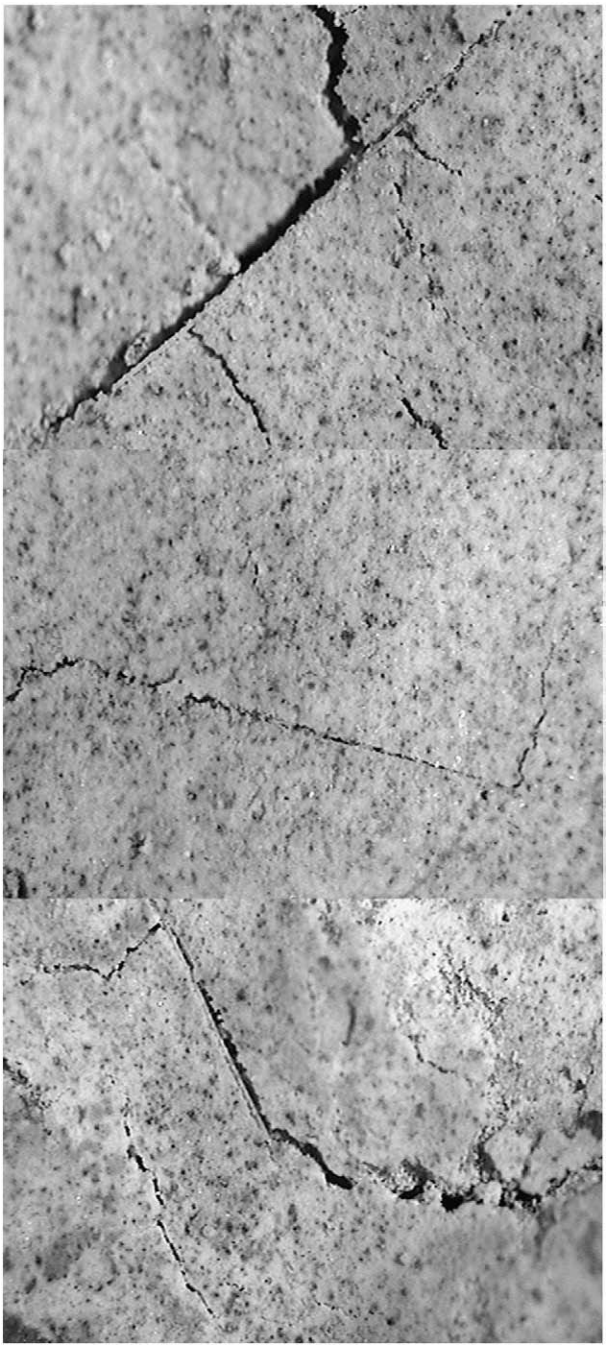

Fig. 2. Micrographies of cracks observed on concrete slab surface in relation to the presence of fibers (cracks have grown parallel to fibers).

As the fibers appeared to be well dispersed in the concrete matrix (no accumulations of fibers were observed) and this second pattern appeared mainly in the surface of the slabs with 900–1000 g/m^3, presenting a loss on cracking control efficiency, it can be inferred that both facts, crack pattern and amount of fiber could be related.

In order to better understand fiber–matrix interaction at early ages and its consequences on cracking control effectiveness, several simple elastic analyses with finite element (FE) models have been performed, considering three different amounts and lengths of two AR-glass fibers.

The aim of this study has been to identify the cracking risks of concrete, associated with drying shrinkage at early ages, induced by the presence of dispersible short AR-glass fibers, trying to better understand the associated phenomena.

2. Fiber–matrix FE models

In order to better understand the results obtained in the experimental tests, several analyses were run on simple FE models. The computer program ANSYS® was used to perform the FE analyses.

Although the interaction between fiber and concrete matrix is a three-dimensional problem, simplified two dimensions FE models were built, considering the fiber dimensions (great length with regard to a much reduced section) and the effect of drying shrinkage on concrete exposed surfaces [5]. The models were therefore meshed with plane elastic elements with thickness for both materials involved: concrete matrix and glass fibers.

The input data needed to run the FE analyses included geometric and mechanical parameters, load applied and boundary conditions.

The geometric parameters were defined considering fiber dimensions and VF fiber included in each case, taking into account the random distribution of fibers. In all cases, fiber dimensions were considered to be those of a single filament. The area of influence of each fiber, calculated for each amount and length of fibers, was modeled as a circular area, placing the fiber in the middle (Fig. 3). This geometry eased the load application and the placement of boundary conditions, with regard to square models [14,15], as it presented two axes of symmetry (which allowed to simplify the model to one fourth) and no corners. Fig. 4 shows the geometry of a FE model considered in these analyses.

The mechanical parameters required were the density, elastic modulus and Poisson coefficient of the fibers and concrete. The fiber parameters can be considered constant during the cement hydration, while concrete parameters varied with time. In order to simulate the non-linear behavior of the concrete matrix at early ages, a sequence of static elastic analyses, considering different elastic moduli of concrete, were run on each FE model.

The load applied on the models simulated the effect of drying shrinkage of concrete at early ages. The load was applied on the model considering a pressure homogeneously distributed on the perimeter of the model (Fig. 4). This simulation effectively produced an isotropic stress field in a reference model (without fibers) which was deformed when a fiber was included. This approach to the application of the load on the model also limited the effects of FE size and shape.

In order to simulate both symmetry axes of the FE models, the boundary conditions applied on the FE nodes located on the axes of the model corresponded to displacement restrictions in the perpendicular direction to the axis and free displacement in the axial direction.

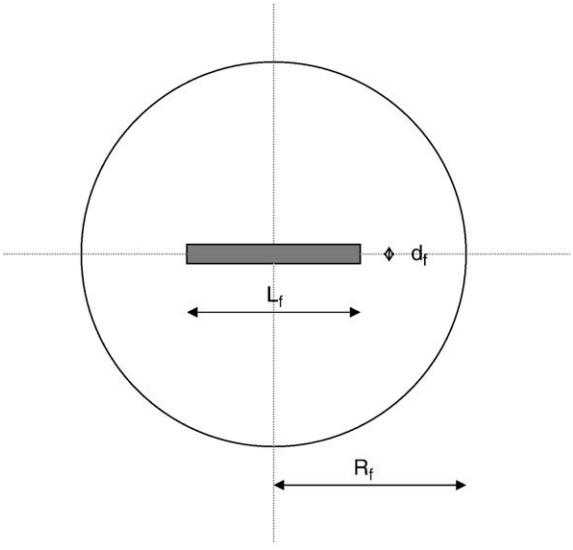

Fig. 3. Basic FE model sketch of a fiber included in a concrete matrix and main dimensions considered (out of scale).

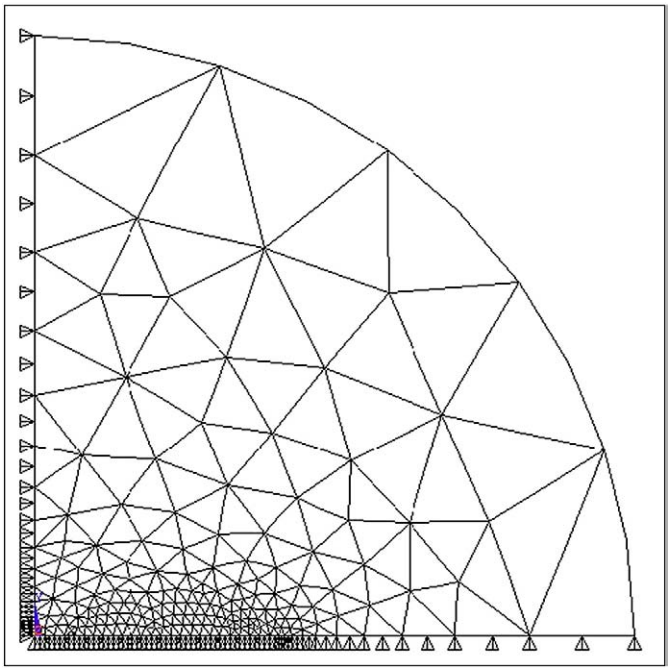

Fig. 4. FE model of a fiber included in concrete simplified considering two axes of symmetry and boundary conditions (1/4 of the basic model).

2.1. FE model parameters

The shape of the FE models was defined as a quarter of cylinder, which simulates concrete matrix, where a quarter of glass fiber is included. The cylinder height corresponds to the diameter of the fiber (13 μm) and the radius of the cylinder depended on the length and amount of fibers included (related to VF, considering fiber density). Table 1 presents the parameters considered and the results obtained using Eq. (1):

$$R = \sqrt{\frac{L_f \cdot d_f \cdot \rho_f}{\pi \cdot W_f}}. \quad (1)$$

Where L_f is the fiber length (in mm), d_f is the diameter of the fiber (0.013 mm), ρ_f is the glass fiber density (2.58 g/cm^3) and W_f is the amount of fiber included (in kg of fiber per liter of concrete).

FE models were built considering two variables in order to identify their influence on cracking risk of concrete matrix at early ages:

a) W_f, amount of glass fiber included: 600, 900 and 1200 g of fiber (12 mm length) per cubic meter of concrete.
b) L_f, glass fiber length: 6, 12 and 18 mm (600 g of fiber per cubic meter of concrete).

The mechanical parameters of the glass fibers considered for the FE models were: a density of 2.58 g/cm^3, a Poisson coefficient of 0.3 and two elastic moduli, 70 and 40 GPa. The first value corresponded to the glass fiber modulus and the second represented the softening effect of the fiber sizing on the fiber mechanical performance, because the fiber coating can produce changes in the fiber surface chemical and nanomechanical properties which modify the interface stiffness [11,16].

Table 1
Geometric parameters of the FE models.

Model	Glass fiber weight (g/m^3)	Volumetric fraction (%)	Fiber length (mm)	Area of influence (mm^2)	Radius (mm)
V6–GP6	600	0.023256	6	335.4	10.33253
V6–GP12	600	0.023256	12	670.8	14.6124
V6–GP18	600	0.023256	18	1006.2	17.89647
V6–GP12	600	0.023256	12	670.8	14.6124
V9–GP12	900	0.034884	12	447.2	11.93098
V12–GP12	1200	0.046512	12	335.4	10.33253

The mechanical parameters considered for the concrete were a density of 2.3 g/cm^3, a Poisson coefficient of 0.2 and a sequence of elastic moduli from 0.5 up to 8 GPa. This sequence simulated the evolution of concrete mechanical properties at early age (up to 24 h) [5,17,18].

The load applied consisted on a homogeneous pressure of 1 MPa on the perimeter of the model. The results obtained in the reference model (no fiber and a load of 1 MPa applied homogeneously distributed on the perimeter) produced an isotropic stress field of 1 MPa and, consequently, no shear stress.

All the models with fiber included reproduced the same load state and the results reported were always referred to as a ratio (stresses with regard to 1 MPa). Therefore, all the values of stress over 1 MPa implied an increase of cracking risk which would be related to fiber presence in concrete matrix.

3. Results of the FE models

Five different FE models were built, considering three VF fiber and three fiber lengths, as described previously. In the first case, the influence of VF is evaluated, in order to compare FE results with the experimental results, searching for a correspondence with the variation of cracking control effectiveness experimentally measured. In a second stage, FE models were used to evaluate cracking risks derived from fiber presence in the concrete matrix related to fiber length.

Each model has been analyzed considering two fiber elastic moduli and twelve concrete elastic moduli, simulating fiber coating softening effect and matrix rigidization due to cement paste hydration, respectively. Altogether, one hundred and twenty FE analyses were performed.

The results obtained from the computer analyses consisted of numerical results of stresses on the FE nodes on the direction of the fiber, perpendicular to the fiber and shear stresses, and graphics of the stress state of the model. Fig. 5A and B shows the general behavior and the stresses distribution observed on the FE models. Fig. 5A displays the stress distribution obtained on the FE analyses in the perpendicular direction to the fiber, and Fig. 5B presents the shear stress distribution. It can be observed that the presence of fibers produces an increase of tension stress in the matrix around the fiber and shear stresses appearance. Fig. 6A and B represents in detail the stress distribution and a stress vectorization, respectively. The maximum tension was measured on the nodes located on the fiber–concrete interface, due to the different mechanical performances of both materials. The stress vectorization indicates that the presence of the fiber produces a deformation of the stress field. Fig. 7 represents a sketch of the stress field deformation.

3.1. FE models with different fiber volumetric fractions (VF)

The maximum tension stress ratio in the perpendicular direction to the fiber (σmax/σ_{ref}; σ_{ref} = 1 MPa), considering three different VFs of two types of glass fibers (with and without coating) of length 12 mm and the stiffening process due to concrete matrix hydration, are summarized in Fig. 8. It must be highlighted that any value over 1 MPa implies an overstress of the concrete matrix and, therefore, an increase of the cracking risk.

All curves representing the models' behavior exhibit the same pattern: a first stage where the stress ratio decreases rapidly, reaching a minimum stress ratio around 1.06; a second stage characterized by a

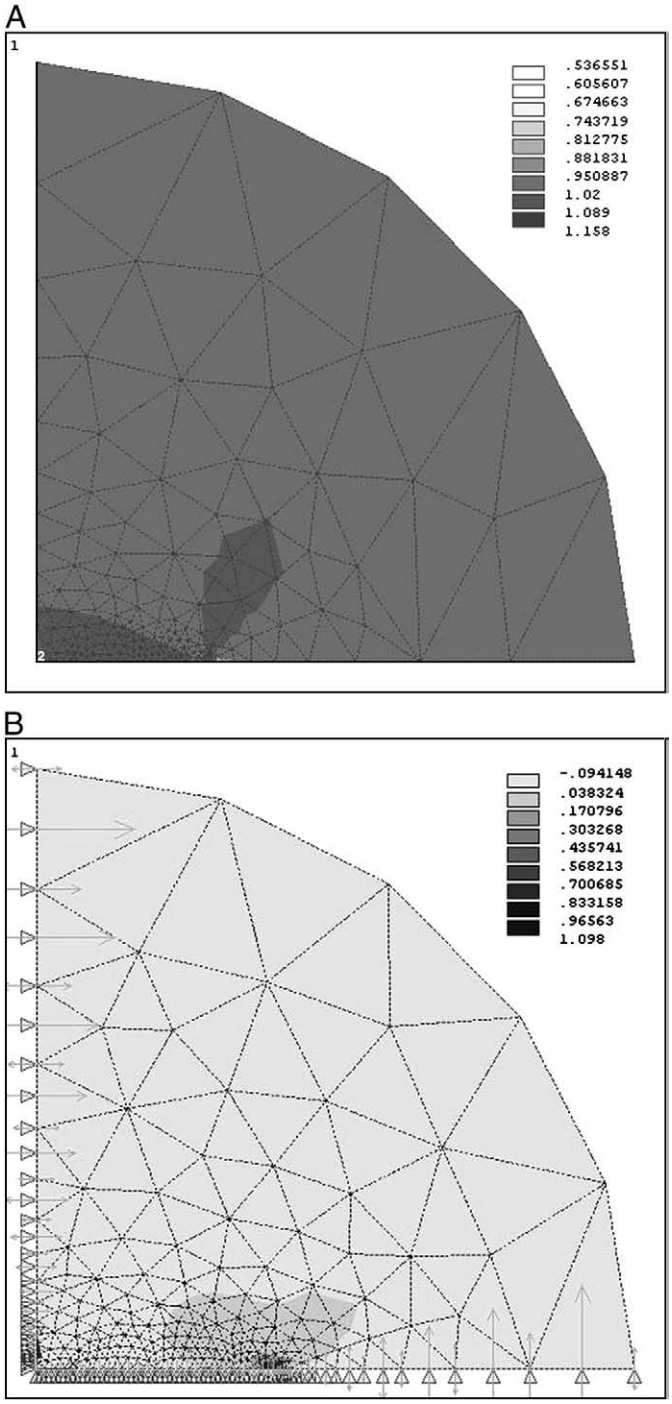

Fig. 5. Distribution of stresses on the FE models: (A) in the perpendicular direction to the fiber (axis *Y*) and (B) shear stress.

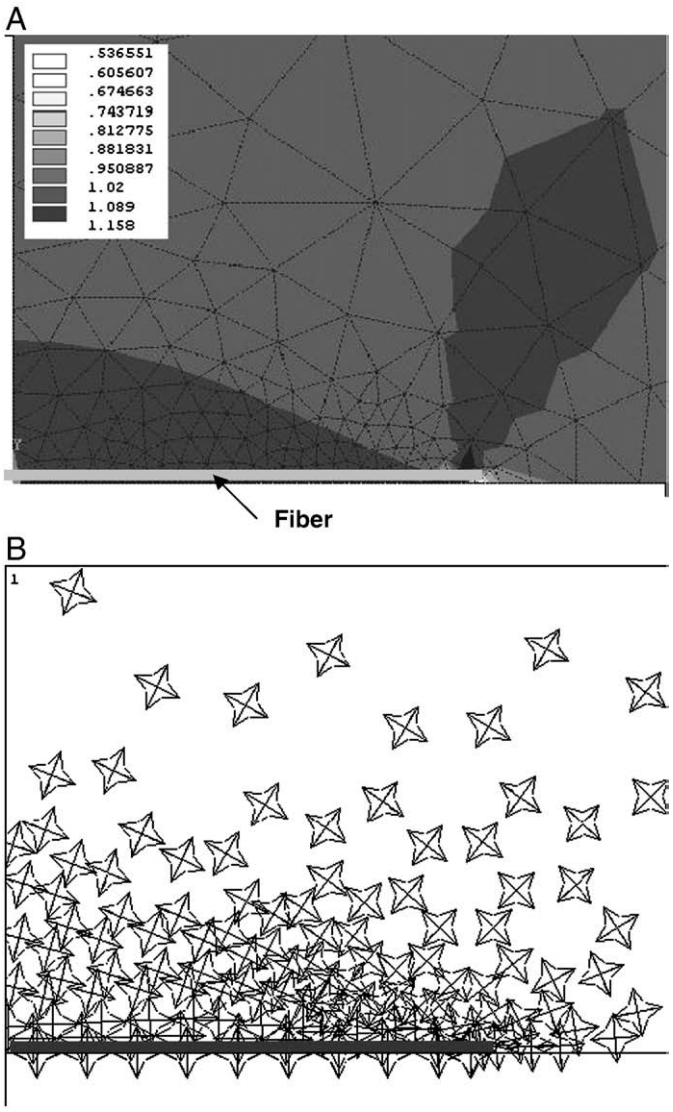

Fig. 6. Detail of the stress distribution on the FE model: (A) stress quantification and (B) vectorization of stress results.

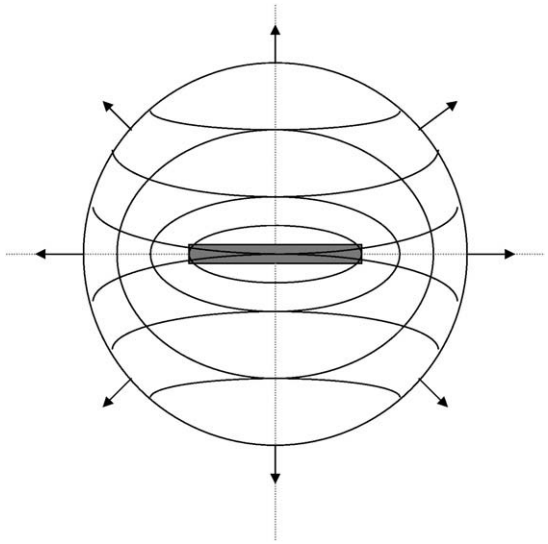

Fig. 7. Stress distribution sketch on the FE model. The presence of the fiber modifies the stress field on the matrix around the fiber.

fast increase reaching a maximum value at a modulus ratio of 0.1 and; a third stage that shows a slight decrease. The maximum value of stress ratio is achieved for 900 g of fiber, and it reaches a stress ratio of 1.15, which implies an overstress of 15% on the concrete matrix due to VF fiber.

Fig. 9 presents the maximum shear stress ratio (τ_{max}/σ_{ref}; σ_{ref} = 1 MPa) for different VFs and concrete moduli. In all cases a fast decrease of shear stress happened during the first stage of the stiffen process according to a potential function. No significant differences can be observed with regard to VF fiber. In both cases – tension and shear stresses – the models with the same VF fiber and different fiber moduli plot coincident curves, considering modulus ratio.

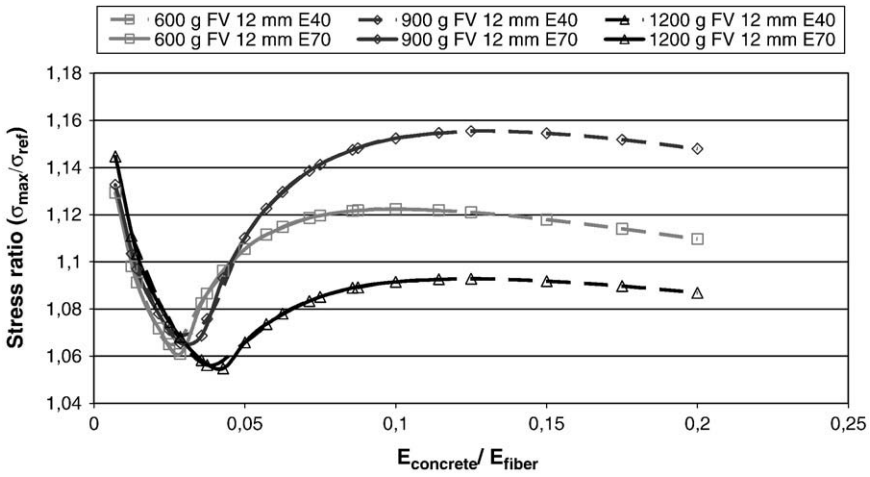

Fig. 8. Maximum stress ratio perpendicular to the fiber during concrete setting, considering Young modulus of concrete to fiber ratio, for different amounts of 12 mm fiber.

3.2. FE models with different fiber lengths

Fig. 10 records the maximum tension stress ratio in the perpendicular direction to the fiber, considering 600 g of three different fiber lengths of two types of glass fibers (with and without coating) and the stiffening process due to concrete matrix hydration. All the stress ratio curves follow the same pattern described previously, but the change in length modifies the maximum value and the modulus ratio when it occurs.

The maximum value of tension stress ratio is achieved for the fiber of 18 mm length, and reaches 1.19 MPa, which implies an overstress of 19% on the concrete matrix due to VF fiber. It appears for a modulus ratio ($E_{concrete}/E_{fiber}$) of 0.05. The fiber of length 12 mm reached 1.12 at a modulus ratio of 0.1. At last, the 6 mm long fiber reached 1.09 at 0.12.

Fig. 11 presents the maximum shear stress ratio for different fiber lengths and concrete stiffness. In all cases a fast decrease of shear stress happened during the first stage of the stiffening process, according to a potential function. Slight differences can be observed considering that the lower the modulus ratio, the larger the difference. On the other hand, the shorter the fiber length, the larger the shear stress.

4. Discussion

The results obtained indicate that the stress distribution of concrete matrix is modified by the presence of the VF and the fiber lengths at early age.

Although shrinkage and cracking are related, cracking can occur with different values than those of shrinkage, as early age shrinkage combines autogenous (related to cement paste hydration, that also relates to concrete stiffening) and drying shrinkage (not related to cement hydration and, therefore, neither to concrete properties evolution). Depending on which type governs shrinkage, there would be more relation between them. In this study, drying was considered the main cause of shrinkage.

In the case of concrete without fibers, the combination of shrinkage and concrete stiffening produces tension stress in the concrete matrix. Shrinkage and the evolution of concrete mechanical properties can be assumed to be the same in any direction considered (on the same exposed surface, if related to drying shrinkage). Therefore, the cracking risk can be assumed to be also isotropic.

Consequently, the strain field produced by shrinkage is isotropic and, when plain concrete mechanical properties evolve, it creates an isotropic stress field, until the first crack appears. According to this, in

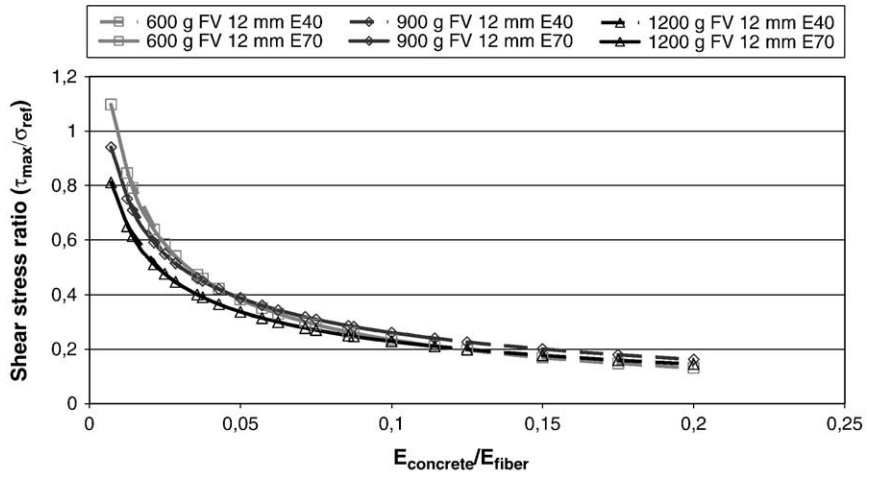

Fig. 9. Maximum shear stress (regarding 1 MPa stress field) during concrete setting, considering Young modulus of concrete with regard to fiber ratio, for different amounts of 12 mm glass fiber.

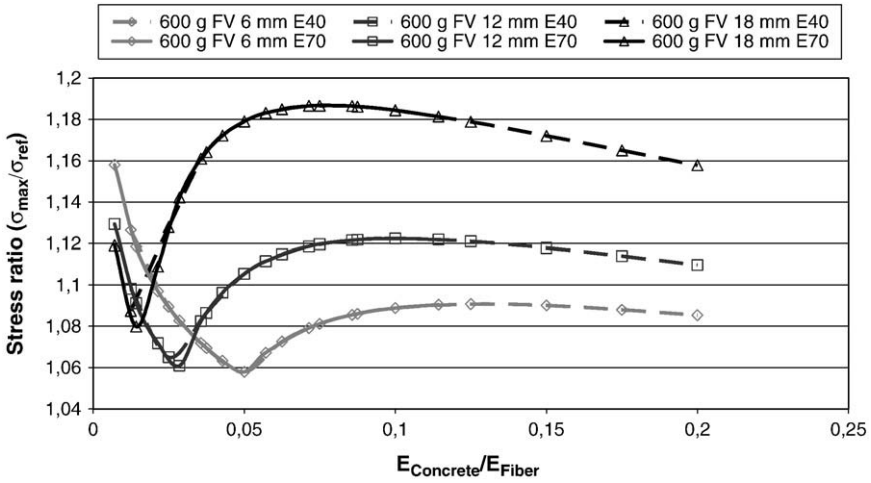

Fig. 10. Maximum stress ratio perpendicular to the fiber during concrete setting, considering Young modulus of concrete to fiber ratio, for different fiber lengths.

the experimental program reported [6], cracking observed in plain concrete specimens has no main direction (mapped cracking).

When short fibers are added to concrete, the strain field remains isotropic (fibers do not modify shrinkage significantly), while the stress produced depends on the direction considered, modifying the stress field. It must be highlighted that the inclusion of fibers produces shear stresses in the concrete matrix, due to the different mechanical stiffnesses.

The interface between fiber and concrete evolves with time, as concrete matrix properties increase. Figs. 5A, B and 6A, B show that the maximum values of stress appeared in the interface between fiber and concrete, at a certain distance from the edge of the fiber. This length is related to the interfacial length needed to transmit tensional stress on the fiber to the cement matrix [10].

The results of maximum stress ratio for different VF fibers, can explain the anomalous behavior observed for certain fiber amounts in the previous experimental program.

The curves of stress ratio with regard to modulus ratio present three stages, as shown in Figs. 8 and 10. At very early ages, concrete behaves plastically and relaxes stress due to creep. Cracking risks at very early ages can be considered very reduced, as modulus ratio is very low. Consequently, the first stage of the pattern curve has negligible influence in cracking risk of concrete.

On the contrary, the maximum value of the stress ratio, at the end of the second stage, conditions the cracking risk due to shrinkage at early ages. Considering 50% of stress relaxation due to creep effects and a double linear logarithmic model of concrete properties evolution [17,18], the concrete modulus for the maximum cracking risk will be between 2 and 8 GPa, depending on the type of concrete considered. For these values, the maximum stress ratio on the models under study is reached.

The results obtained can be applied on any type of concrete, as concrete modulus always evolves from zero to the hardened concrete modulus and the models presented refer to modulus ratio (it is an independent variable). To reproduce a certain concrete, concrete modulus must be adjusted with time.

The results also confirmed that more fiber does not mean a better cracking control, as it was demonstrated in the experimental study. For 600 g/m^3 of fiber (per cubic meter of concrete), the maximum value of tension stress in the perpendicular direction to the fiber increases 12% with regard to plain concrete, while for 900 g/m^3 it reaches 15% and for 1200 g/m^3 barely reaches 10%.

In the moment when the maximum value of tension stress occurred, shear stress reaches 20% of tension stress, increasing the stress intensity of the matrix and, therefore, the cracking risk. The results of these analyses matched the experimental results [6].

The time when the maximum tension stress happens does not depend on the VF fiber, but on the fiber length and sizing. The inclusion of fiber coating can modify the interphase stiffness. This effect has been simulated in the model as a change on fiber modulus, which brings forward stress curve. At this moment, the concrete still behaves plastically and can relax stress easily. As a result, cracking risk

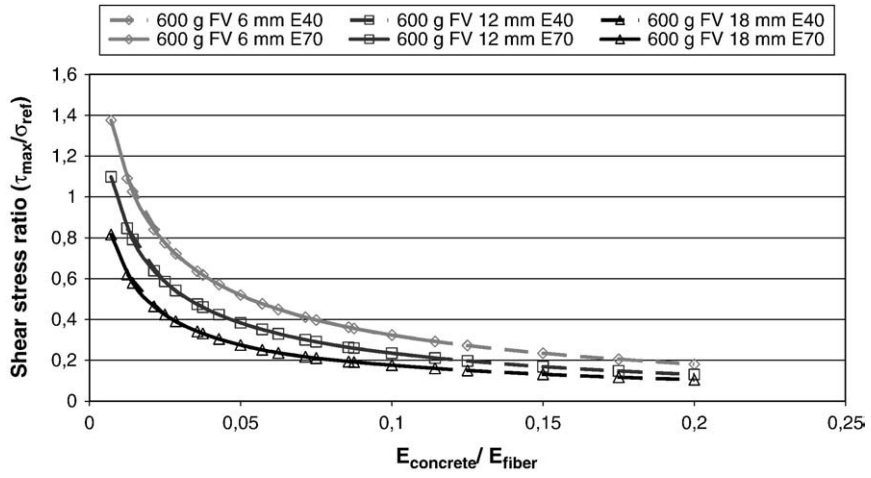

Fig. 11. Maximum shear stress (with regard to 1 MPa stress field) during concrete setting, considering Young modulus of concrete to fiber ratio, for different fiber lengths.

is reduced. It can be assumed that the later the maximum tension stress is reached, the larger the cracking risk, because the concrete matrix is less plastic, increasing concrete modulus without increasing concrete strength significantly [1,16,17].

Fiber length has been also studied to evaluate its influence on cracking risk at early ages. Up to the results obtained in this study, it has been demonstrated that the larger the fiber length, the larger the tension stress and the cracking risk. For 6 mm fiber length, the maximum tension stress increase reached 9%, while for 9 mm was 12% and for 18 mm increase to 19%.

In this study, a homogeneous random distribution of fibers was assumed. If fiber accumulations appear, due to poor mixing, the influence surface of every fiber would be reduced, increasing tension stress and cracking risk.

Considering the evolution of fiber–concrete interface regarding concrete properties, fiber length and VF, the design of fiber coating could be a technological solution to overcome the problems that appeared due to fiber matrix interaction at early ages.

5. Conclusions

In this paper, fiber–matrix interaction is analyzed considering different amounts (from 600 to 1200 g/m^3) and lengths (6, 12 and 18 mm) of AR-glass fibers and two different fiber coatings. The study combines experimental results and analyses with simple FE models to reach a better understanding of early age concrete behavior.

As far as the results obtained are consequent with some simplifications, and according with the experimental data obtained in a previous experimental program, some main conclusions can be drawn:

- The inclusion of low VF of short fiber is an effective measurement to control early age cracking. For some VF and fiber length, the reduction of cracked area reaches up to 95%.
- The inclusion of fibers in the concrete matrix deforms the stress field created by the combination of shrinkage and cement paste hydration at early ages. This deformation produces an increase of tension stress in the concrete–fiber interface and shear stresses appear on the extremes of the fiber (anchorage length).
- The increase of stress at early ages enlarges cracking risk due to shrinkage and fiber matrix interaction. The stress intensity depends on the VF fiber and length, combining geometric and mechanical parameters.
- The stress state on the fiber matrix interface depends on the concrete mechanical properties evolution (grade of hydration) and fiber mechanical properties (constitutive material and sizing amount and type).
- The VF fiber modifies the cracking risk: among the amounts considered in this study, 900 g/m^3 produces maximum tension stress in the perpendicular direction to the fiber. These results match the experimental results previously published.
- Fiber length influences stress intensity and the moment when maximum values appear. Among the fiber lengths considered in this study, the shorter the length, the lower the stress. Experimental results are needed to confirm this assertion.
- Fiber modulus also influences the interfacial stress development, but it does not influence stress intensity. The lower the modulus, the sooner the stress develops, and, therefore, the lower the cracking risk, as concrete has larger creep ability at very early ages that can relax stress easier.

Acknowledgements

The author wants to acknowledge the kind advice given by Prof. Francisco Hernandez-Olivares, the language revision done by Prof. Isabel Salto Weis and also the financial support given for the experimental program by the AR glass fiber manufacturer, Saint Gobain-Vetrotex España, S.A.

References

[1] S. Altoubat, D. Lange, Early Age Stresses and Creep–Shrinkage Interaction of Restrained Concrete, COE Report 14 for FAA, 2001.
[2] W.J. Weiss, in: A. Bentur (Ed.), Experimental Determination of the "Time-Zero t0" (Maturity-Zero M0), Chapter 6.1 in Early Age Cracking in Cementitious Systems, RILEM State of the Art Report TC-EAS, 2002.
[3] E. Holt, M. Leivo, Cracking risks associated with early age shrinkage, Cement and Concrete Composites 26 (5) (2004) 521–530.
[4] W. J. Weiss, Early-Age Shrinkage Cracking In Concrete, Ph D thesis, Northwestern University, (1999).
[5] H. Mihashi, J.P. Leite, State of the art report on control of cracking in early age concrete, Journal of Advanced Concrete Technology 2 (2) (2004) 141–154.
[6] G. Barluenga, F. Hernández-Olivares, Cracking control of concretes modified with short AR-glass fibers at early age: experimental results on standard concrete and SCC, Cement and Concrete Research 37 (12) (2007) 1624–1638.
[7] F.A. Mirza, P. Soroushian, Effects of alkali-resistant glass fiber reinforcement on crack and temperature resistance of lightweight concrete, Cement and Concrete Composites 24 (2) (2002) 223–227.
[8] H.A. Mesbah, F. Buyle-Bodin, Efficiency of polypropylene and metallic fibres on control of shrinkage and cracking of recycled aggregate mortars, Construction and Building Materials 13 (1999) 439–447.
[9] N. Banthia, R. Gupta, Influence of polypropylene fiber geometry on plastic shrinkage cracking in concrete, Cement and Concrete Research 36 (7) (2006) 1263–1267.
[10] S. Zhandarov, E. Mäder, Characterization of fiber/matrix interface strength: applicability of different tests, approaches and parameters, Composites Science and Technology 65 (2005) 149–160.
[11] S.L. Gao, E. Mäder, R. Plonka, Coatings for glass fibers in a cementitious matrix, Acta Materialia 52 (2004) 4745–4755.
[12] C. Schefflera, S.L. Gao, R. Plonka, E. Mäder, S. Hempel, M. Butler, V. Mechtcherine, Interphase modification of alkali-resistant glass fibres and carbon fibres for textile reinforced concrete I: fibre properties and durability, Composites Science and Technology 69 (2009) 531–538.
[13] T. Desai, R. Shah, A. Peled, B. Mobasher, Mechanical properties of concrete reinforced with AR-glass fibers, 7th International Conference on Brittle-Matrix Composites, BMC-7, Warsaw, Poland, October 13–15th, 2003.
[14] W. Yang, W.J. Weiss, S.P. Shah, Predicting shrinkage stress field in concrete slab on elastic subgrade, Journal of Engineering Mechanics 126 (1) (2000) 35–42.
[15] D. Cusson, Sensitivity analysis of the early-age properties of high-performance concrete — a case study on bridge barriers, 6th Int. Conference on Creep, Shrinkage and Durability of Concrete and other Quasi-brittle materials, Cambridge MA, 2001.
[16] V.C. Li, On engineered cementitious composites (ECC). A review of the material and its applications, Journal of Advanced Concrete Technology 1 (3) (2003) 215–230.
[17] M. Larson, J.E. Jonasson, Linear logarithmic model for concrete creep. I. Formulation and evaluation, Journal of Advanced Concrete Technology 1 (2) (2003) 172–187.
[18] M. Larson, J.E. Jonasson, Linear logarithmic model for concrete creep. II. Prediction formulas and description of creep behaviour, Journal of Advanced Concrete Technology 1 (2) (2003) 188–200.